

Linear optical and quadratic electro-optic response of carbon nanotubes: universal analytic expressions for arbitrary chirality

This article has been downloaded from IOPscience. Please scroll down to see the full text article.

2008 J. Phys.: Condens. Matter 20 275211

(<http://iopscience.iop.org/0953-8984/20/27/275211>)

View [the table of contents for this issue](#), or go to the [journal homepage](#) for more

Download details:

IP Address: 129.252.86.83

The article was downloaded on 29/05/2010 at 13:24

Please note that [terms and conditions apply](#).

Linear optical and quadratic electro-optic response of carbon nanotubes: universal analytic expressions for arbitrary chirality

Abbas Zarifi and Thomas Garm Pedersen

Department of Physics and Nanotechnology, Aalborg University, DK-9220, Aalborg East, Denmark

E-mail: zarifi@nano.aau.dk

Received 16 February 2008, in final form 14 May 2008

Published 3 June 2008

Online at stacks.iop.org/JPhysCM/20/275211

Abstract

Using a universal density of states (Mintmire and White 1998 *Phys. Rev. Lett.* **81** 2506), we have found an analytic expression for the long-axis linear susceptibility of single-walled carbon nanotubes valid for arbitrary diameter and chirality. The applicability of our general expression has been assessed by comparison with numerical calculations. Excellent agreement is demonstrated in the low-energy range for semiconducting carbon nanotubes having a moderate or large diameter. The agreement is less convincing for metallic nanotubes having the same diameter as semiconducting ones and the reason for this difference has been clarified. Based on the simple closed-form expression for the linear susceptibility and using the perturbation treatment developed by Aspnes and Rowe (1972 *Phys. Rev. B* **5** 4022), an analytic expression for the third-order nonlinear optical susceptibility $\chi^{(3)}(\omega; 0, 0, \omega)$ has been derived for arbitrary semiconducting single-walled carbon nanotubes.

1. Introduction

Single-walled carbon nanotube (CN) structures, constructed by rolling up a graphite sheet into a cylinder, can be specified by a pair of indices (n, m) with $2n + m = 3p + r$, where p is an integer and $r = 0, 1, 2$ define metallic, semiconducting type I (SI), and type II (SII) CNs, respectively [1–3]. Since their discovery in 1991 [4], the electronic properties of these structures have attracted much attention. Their electronic properties within the single-particle approximation are often described by the tight-binding approximation [5–9]. The optical properties of CNs have been examined in several theoretical and experimental papers [10–14]. In our previous work [15] we used a simple orthogonal tight-binding model to study the dipole matrix element and linear susceptibility for light polarized parallel and perpendicular to the nanotube axis. We found an analytic expression for the linear susceptibility of zigzag CNs in the parallel case. By studying the optical absorption of CNs, Malić and co-workers have also presented an analytic expression for the absorption coefficient of zigzag CNs [16]. However, due to the rather complicated k -dependence of the energy, it has not yet been possible to find analytic results for the optical properties of arbitrary

(n, m) chiral CNs. In this paper, we demonstrate that an approximate optical susceptibility $\chi(\omega)$ of arbitrary CNs can be obtained. Importantly, excellent agreement with full numerical results is found in the low-energy range. A central ingredient in the present computation is the universal density of states (DOS) found by White and Mintmire [17, 18]. Using a first-order expression for the energy, these authors showed that all semiconducting CNs with similar diameters have similar DOS near the Fermi level, independent of chiral angle. We demonstrate that this observation combined with an approximation of the CN dipole matrix elements near the Fermi level enables analytic integration over all transition energies. The resulting analytic expression for the linear susceptibility provides an accurate closed-form expression valid for CNs with arbitrary diameter and chirality.

The paper is organized as follows. In section 2, we discuss the energy dispersion relation and optical matrix elements of chiral CNs in a convenient rotated coordinate system. Expanding the optical matrix element close to the Fermi level and using the universal DOS we derive a closed-form expression for linear susceptibility for arbitrary (n, m) CNs and explain its dependency on the structure parameters in section 3. We use the linear susceptibility to derive an analytic

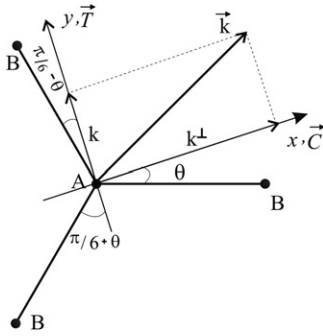


Figure 1. Positions of an A atom at the origin and its three nearest neighbor B atoms. The angle between these bonds and the chiral \vec{C} and translational \vec{T} vectors are also shown.

expression for the quadratic electro-optic (QEO) response for arbitrary (n, m) semiconducting CNs in section 4. Finally, a summary is given in section 5.

2. Theory

Figure 1 shows the atom A at the origin and its three nearest neighbor B atoms in the hexagonal lattice of graphene along with the rotated coordinate system (x, y) that we use for our analytic calculations.

To make a tube, the translational vector \vec{T} will be in the direction of the nanotube axis and the chiral vector \vec{C} in the circumferential direction. Hence, we consider the y axis parallel to the translational vector and the x axis in the circumferential direction in order that the wavenumbers k and k^\perp provide the axial and circumferential components of the wavevector, respectively. Following [1], the elements of the Hamiltonian matrix \vec{H} are given by

$$H_{\alpha\beta}(k) = \sum_t e^{i\vec{k}\cdot(\vec{R}_{\beta 0} - \vec{R}_{\alpha t})} \left\langle \varphi(\vec{r} - \vec{R}_{\alpha t}) \left| H \right| \varphi(\vec{r} - \vec{R}_{\beta 0}) \right\rangle. \quad (1)$$

Here, $\vec{R}_{\alpha t}(\vec{R}_{\beta 0})$ is the position vector for each $\alpha(\beta)$ carbon atoms in the t th (zeroth) unit cell, $\varphi(\vec{r} - \vec{R})$ denotes the atomic π orbital of each carbon atom, and H is the Hamiltonian. The elements of the 2×2 Hamiltonian matrix are defined by

$$\begin{aligned} H_{12} = H_{21}^* &= \gamma_0 [e^{-i2K_1/3} + 2e^{iK_1/3} \cos(K_2)] \\ H_{11} = H_{22} &= 0 \\ K_1 &= [k^\perp \cos(\theta) - k \sin(\theta)] \sqrt{3}a/2 \\ K_2 &= [k^\perp \sin(\theta) + k \cos(\theta)] a/2, \end{aligned} \quad (2)$$

where $\theta = \pi/6 - \cos^{-1}[(2n + m)/2\sqrt{n^2 + m^2 + nm}]$, $\gamma_0 \approx 2.89$ eV is the nearest neighbor overlap integral and $a = 2.46$ Å is the lattice constant of two-dimensional graphite [1]. Solving the secular equation, the energy eigenvalues are obtained as a function of θ, k :

$$\begin{aligned} E_{c,v}(k) &= \pm E(k), \\ E(k) &\equiv \gamma_0 \sqrt{3 + 2 \cos(2K_2) + 4 \cos(K_2) \cos(K_1)}, \end{aligned} \quad (3)$$

where the negative and positive solutions provide valence (v) and conduction (c) band energies, respectively. The corresponding normalized eigenvectors are given by

$$\begin{aligned} \vec{v}(k) &= \frac{1}{\sqrt{2}}(-g(k), 1) \\ \vec{c}(k) &= \frac{1}{\sqrt{2}}(g(k), 1) \\ g(k) &= \frac{\gamma_0 e^{-i2K_1/3}}{E(k)} [1 + 2e^{iK_1} \cos(K_2)]. \end{aligned} \quad (4)$$

In the case of parallel polarization, the direction of the electric field is in the direction of the nanotube axis. Using equation (8) in [15], the axial (y) component of the dipole matrix element is given by

$$d_{cv}^y(k) = \frac{-e}{E_{cv}(k)} \sum_{\alpha,\beta} c_{\alpha}^*(k) v_{\beta}(k) \frac{1}{i} \frac{dH_{\alpha\beta}}{dk}, \quad (5)$$

where $e > 0$ is the elementary charge and $E_{cv}(k) = E_c(k) - E_v(k) = 2E_c(k)$. Inserting the eigenvector equations (4) into equation (5), the dipole matrix element for light polarized parallel to the nanotube axis is given by

$$\begin{aligned} d_{cv}^y(k) &= \frac{2ea\gamma_0^2}{\sqrt{3}E_{cv}^2(k)} [\sin(\theta) \{\cos(2K_2) - \cos(K_2) \cos(K_1)\} \\ &\quad + \sqrt{3} \cos(\theta) \sin(K_2) \sin(K_1)]. \end{aligned} \quad (6)$$

Introducing $K_2 = k_y a/2$ and $K_1 = \sqrt{3}k_x a/2$, equation (6) gives equation (11) in [19]. The difference between our method and that of [19] is that in our rotated coordinate system x and y are always circumferential and longitudinal coordinates. Moreover, it demonstrates that the optical matrix element for the two nearest neighbor atoms introduced in [19] is given by $M = 2a\gamma_0 m_e / (\sqrt{3}\hbar^2)$. For all arbitrary (n, m) semiconducting CNs, the allowed wavevector components k_μ^\perp in the circumferential direction are defined by

$$k_\mu^\perp L = 2\pi\mu, \quad \mu = 0, \dots, N-1, \quad (7)$$

where L is the length of the nanotube circumference and N the number of hexagons in the nanotube unit cell. For zigzag nanotubes ($\theta = \pi/6$), equation (6) yields equation (9) in [15] and for armchair nanotubes ($\theta = 0$), it yields equation (12) in [19]. Note that in [19], $D(k)$ denotes the momentum matrix element, which is defined by $D_{cv}(k) = mE_{cv}d_{cv}(k)/\hbar^2 e$.

3. Linear susceptibility

To compute the long-axis linear susceptibility (χ_{yy}) of CNs, we start with equation (2) in [15] written in the following form:

$$\chi_{yy}(\omega) = \frac{2}{\pi \epsilon_0 \sigma} \sum_{c,v} \int_{-\pi/T}^{\pi/T} |d_{cv}^y(k)|^2 \frac{E_{cv}(k) dk}{E_{cv}^2(k) - \hbar^2 \Omega^2}. \quad (8)$$

Here, the nanotube cross sectional area $\sigma = \pi R^2$, where R is the radius of a CN, ϵ_0 is the vacuum permittivity, T is the length of the unit cell and $\Omega = \omega + i\Gamma$ contains the

photon frequency ω and the broadening parameter Γ . As mentioned in [15], the dimensionless susceptibility $\chi_{yy}(\omega)$ is introduced by normalizing the polarizability by the cross sectional area of a CN. Using equation (8), we have previously found an analytic expression for the linear susceptibility of zigzag CNs [15]. As a prerequisite, an analytical DOS for zigzag CNs was obtained in order to convert the k -integral into one over energy. Unfortunately, no exact analytic solution for the DOS for arbitrary CNs has been obtained so far. Hence, we utilize a universal but approximate DOS for CNs obtained by Mintmire and White [18] to find an analytic expression for the linear susceptibility of CNs valid in the low photon-energy range. Also, our calculation is simplified by expanding the trigonometric terms in the dipole matrix element equation (6). To this end, we note that the dominant k -vector contributions lie in the vicinity of the K point of the 2D Brillouin zone, i.e. $\vec{K} = (4\pi/3a)[\sin(\theta), \cos(\theta)]$ in the rotated system. Hence, to linear order in $\vec{k} - \vec{K}$, the trigonometric term in equation (6) is given by

$$\begin{aligned} & \sin(\theta) [\cos(2K_2) - \cos(K_2) \cos(K_1)] \\ & + \sqrt{3} \cos(\theta) \sin(K_2) \sin(K_1) \approx \frac{3\sqrt{3}a}{4} \Delta k_\mu^\perp, \end{aligned} \quad (9)$$

where Δk_μ^\perp is the x -component of $\vec{k} - \vec{K}$ given by $\Delta k_\mu^\perp = (2\pi/L)|\mu - 2L \sin(\theta)/3a| = (2\pi/3L)|3\mu - n + m|$ since in the chosen rotated coordinate system $2L \sin(\theta) = a(n - m)$. Equation (9) clearly indicates that in the vicinity of the Fermi level for a CN with an arbitrary chiral angle θ , $d_{cv}^y(k) = 0$ only for the value of the band index $\mu = 2L \sin(\theta)/(3a) = (n - m)/3$. This means that for zigzag ($\theta = 30^\circ$) and armchair ($\theta = 0^\circ$) CNs, the values $\mu = n/3$ and $\mu = 0$, respectively, give a vanishing dipole matrix element. As mentioned above, by using the first-order expression for the energy, $E(k) \approx (\sqrt{3}/2)a\gamma_0\sqrt{\Delta k_\mu^{\perp 2} + \Delta k_\mu^{\parallel 2}}$, Mintmire and White have derived a universal DOS in the vicinity of the Fermi level for all CNs. Following their derivation, the contribution of the band μ at k to the DOS at energy $E(k)$ in the graphene Brillouin zone is given by [18]

$$\frac{dk^\parallel}{dE(k)} = \frac{2E(k)}{\sqrt{3}a\gamma_0\sqrt{E(k)^2 - \varepsilon_\mu^2}}, \quad (10)$$

where

$$\varepsilon_\mu = \frac{\sqrt{3}}{2}a\gamma_0\Delta k_\mu^\perp = \frac{\sqrt{3}\pi a\gamma_0}{L} \left[\mu - \frac{2L}{3a} \sin(\theta) \right]. \quad (11)$$

We note that there is a double degeneracy of bands at low energy for each CN [1]. As a result, to obtain the correct DOS, the contribution of the state at k , equation (10), must be multiplied with a factor of 2. Using equations (9) and (10) and writing $dk^\parallel = (dk^\parallel/dE_{cv})dE_{cv}$ the linear susceptibility is given by

$$\chi_{yy}(\omega) = \frac{6\sqrt{3}e^2a^3\gamma_0^3}{\pi\varepsilon_0\sigma} \sum_{\mu=0}^{N-1} |\Delta k_\mu^\perp|^2 \chi_{yy}^{(\mu)}(\omega), \quad (12)$$

where

$$\chi_{yy}^{(\mu)}(\omega) = \int_{2\varepsilon_\mu}^{\infty} \frac{dE_{cv}}{E_{cv}^2 (E_{cv}^2 - \hbar^2\Omega^2) \sqrt{E_{cv}^2 - 4\varepsilon_\mu^2}}. \quad (13)$$

Here, the integration range $0 \leq \Delta k^\parallel \leq \pi/T$ is now transformed to an integration over E_{cv} . The lower limit $2\varepsilon_\mu$ is the band gap located at $\Delta k^\parallel = 0$ and the upper limit has been approximated by infinity. Alternatively, an upper limit could be determined by requiring that the integrated DOS yields the correct number of states. However, the obtained upper limits only affect the response at rather high-photon energies for which the approximations above are anyway questionable. Hence, for simplicity we integrate over the range $2\varepsilon_\mu \leq E_{cv} < \infty$ and thus $\chi_{yy}^{(\mu)}(\omega)$ is finally given by the analytic expression

$$\chi_{yy}^{(\mu)} = \frac{-1}{4\varepsilon_\mu^2\hbar^2\Omega^2} \left[1 - \frac{\sin^{-1}(\alpha)}{\alpha\sqrt{1-\alpha^2}} \right], \quad (14)$$

where $\alpha = \hbar\Omega/(2\varepsilon_\mu)$. Together with equation (12) this closed-form expression gives the linear susceptibility for arbitrary (n, m) CNs in the low-energy range where ε_μ is a function of tube diameter and chirality as well. For armchair nanotubes, the DOS will have two identical contributions at points $K_2 = \pm 2\pi/(3a)$, in the first Brillouin zone. For other metallic CNs this degeneracy is broken because of deviations of the true energy $E(k)$ from radial symmetry near \vec{k}_F , for the two points $K_2 = \pm 2\pi/(3T)$ are not equivalent. As a result, the susceptibility must be multiplied with a factor of 2 for armchair CNs. We emphasize that equation (14) includes intraband transitions for the bands passing through the Fermi point, where subscripts $c = v$ at $\mu = (n - m)/3$. This point appears only for metallic CNs. For intraband transitions, one can show that the Drude conductivity $\sigma_{yy}^{(\text{intra})}(\omega) = -2i\varepsilon_0(\omega + i\Gamma)\chi_{yy}^{(\text{intra})}(\omega)$ (again with a factor of 2 due to degeneracy) is given by

$$\sigma_{yy}^{(\text{intra})}(\omega) = \frac{i16\sqrt{3}e^2\gamma_0a}{\hbar^2L^2(\omega + i\Gamma)}, \quad (15)$$

which is the dominating term at sufficiently low frequencies. Note that interband transitions with $\mu = (n - m)/3$ give zero contribution to the linear susceptibility.

To assess the applicability of the first-order expression for calculating the linear susceptibility of (n, m) CNs, figure 2 shows the imaginary (χ_{yy}'') parts of χ_{yy} for semiconducting (4, 2), (8, 4), and (10, 6) CNs having diameters about 0.41, 0.82, and 1.09 nm respectively and metallic (12, 9), (12, 12), and (21, 9) CNs having diameters about 1.43, 1.63, and 2.08 nm respectively in comparison with a numerical calculation, where the broadening parameter $\hbar\Gamma = 0.1$ eV [12]. As shown, the first two resonance peaks for semiconducting CNs having a moderate or large diameter overlap well within those obtained by numerical calculation but for metallic CNs this agreement is less convincing. The difference between the two groups of semiconducting and metallic CNs will be discussed in the following.

The position of the resonances near the Fermi level can be estimated as follows. According to the first-order expression for the energy, at $\Delta k^\parallel = 0$ and $\Delta k_\mu^\perp = (2\pi/3L)|3\mu - n + m|$,

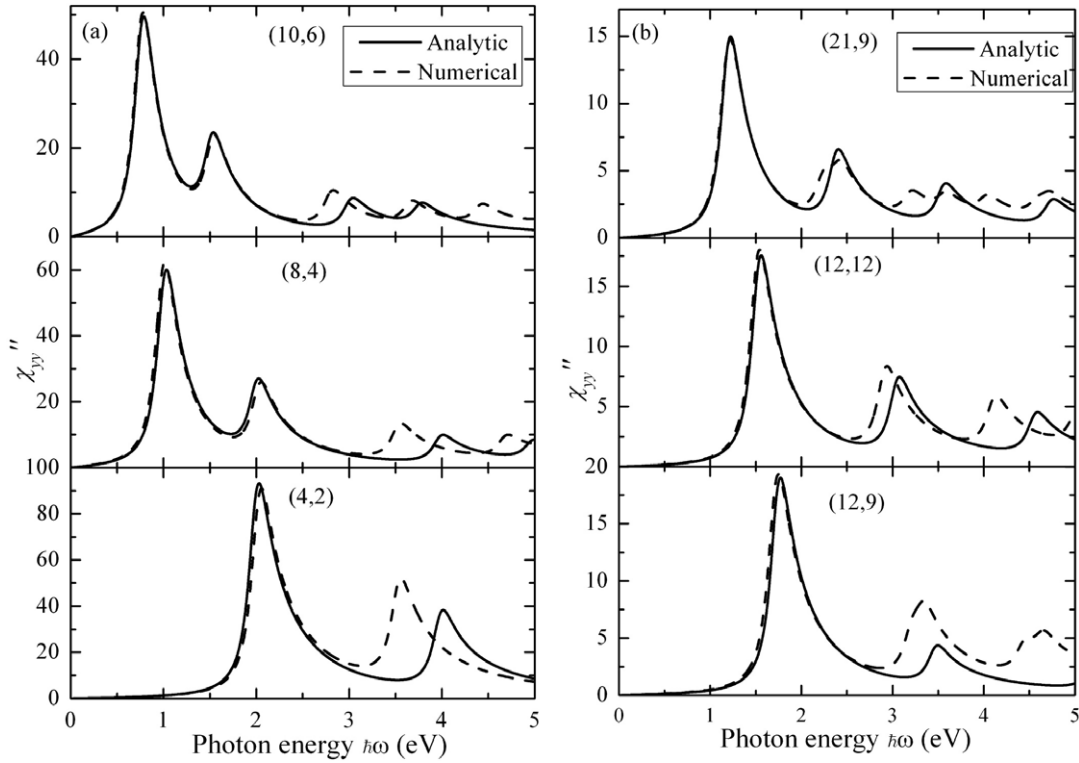


Figure 2. Comparison of analytical and numerical calculations of the interband long-axis linear susceptibility versus energy for semiconducting (a) and metallic (b) CNs.

the value $\mu = (n - m)/3$ gives the Fermi point for metallic CNs. Also, the minimum energy value for the second-lowest conduction band occurs at $\mu = (n - m)/3 \pm 1$ for metallic CNs. For semiconducting CNs, the lowest conduction band is obtained by setting $\mu = (n - m + 1)/3$ and $(n - m - 1)/3$ for SI and SII CNs, respectively. Using these values of μ , the lowest excitation energies for semiconducting (S) and metallic (M) CNs are given by

$$E_{11}^{(S)} = \frac{\sqrt{3}a\gamma_0}{3R}, \quad E_{11}^{(M)} = \frac{\sqrt{3}a\gamma_0}{R}, \quad (16)$$

in agreement with [8]. This equation has been previously obtained by White *et al* [20, 21] by studying the construction of single-walled CNs in terms of their helical and rotational symmetries. Equation (16) shows that the lowest resonance for metallic nanotubes of radius R coincides with that of semiconducting nanotubes of radius $3R$ independent of chirality. This result is only valid in the vicinity of the K point, however. The effect of chirality on the electronic structure and the band gap of single-walled CNs has been studied by White *et al*, see figure 11 and related text in [22]. In agreement with the present work, these authors found that applying the linear approximation for the energy and ignoring curvature effects removes the dependence of van Hove singularities on chirality. Saito and co-workers showed that the peak positions of the van Hove singularities, in fact, depend on the nanotube chirality [8] if corrections beyond the linear approximation are included. They further showed that the trigonal warping effect is larger for metallic than for semiconducting nanotubes of comparable

diameters. The perpendicular components of $\vec{k} - \vec{K}$ for the fundamental resonance of metallic and semiconducting CNs are given by $\Delta k_{\mu}^{\perp(M)} = 1/R$ and $\Delta k_{\mu}^{\perp(S)} = 1/3R$, respectively. Hence, the distance from the K point is three times larger for metallic CNs than for semiconducting CNs. Therefore, interband resonances in metallic CNs rapidly reach the region where the linear approximation is no longer appropriate [8]. This is the reason for the slightly worse agreement between analytic and numerical results for small diameter metallic CNs shown in figure 2. The imaginary (χ''_{yy}) parts of χ_{yy} for several semiconducting CNs having about the same diameter (from 1.08 to 1.09 nm), but different chiral angles, including $\theta = 30^\circ$ for zigzag nanotubes (14, 0) and $\theta = 4.13^\circ$ and 8.2° for chiral nanotubes (9, 7) and (10, 6) respectively, are shown in figure 3(a). Metallic CNs, all having about the same diameter (from 1.35 to 1.41 nm), but different chiral angles, including $\theta = 30^\circ$ for zigzag nanotubes (18, 0), $\theta = 0^\circ$ for armchair nanotubes (10, 10), and $\theta = 9.8^\circ$ for chiral nanotubes (13, 7) are shown in figure 3(b). As shown in figure 3, the chirality dependence of the linear susceptibility is weakly visible for metallic CNs but practically absent for semiconducting CNs.

4. Quadratic electro-optic effect

Using the perturbation treatment developed by Aspnes and Rowe [23], we previously obtained an analytic expression for the quadratic electro-optic (QEO) effect in zigzag CNs [24]. Applying a nonperturbative numerical calculation

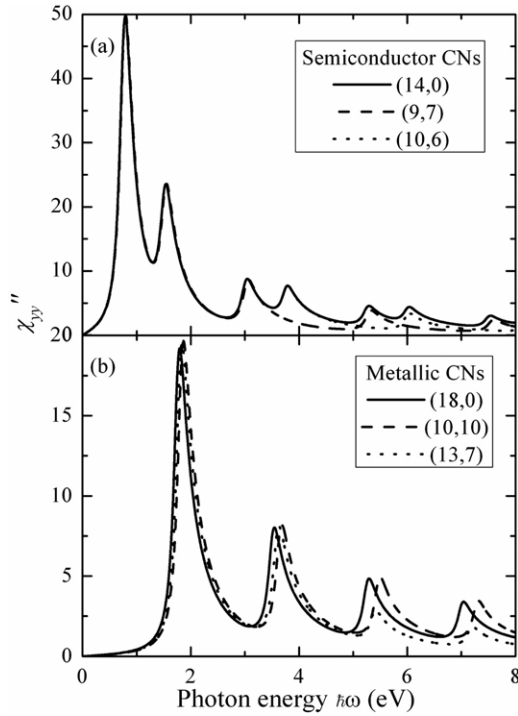


Figure 3. Imaginary part of the interband long-axis linear susceptibility versus energy for several CNs of approximately the same diameter but different chirality. Panel (a) semiconducting CNs and panel (b) metallic CNs.

and comparing with the analytic result, we found a virtually indistinguishable result for zigzag CNs in our previous work [24]. To find the QEO effect in arbitrary (n, m) CNs we

again utilize the approximate relation

$$\chi''_{yy}(\omega; 0, 0, \omega) = \frac{1}{3\hbar^2\Omega^2} \frac{e^2\hbar^2}{8m^*} \frac{\partial^3 [\hbar^2\Omega^2 \chi_{yy}(\omega)]}{\partial(\hbar\Omega)^3}, \quad (17)$$

where m^* is the reduced effective mass. For both numerical and analytic calculations for semiconducting CNs we use the effective mass related to the fundamental valence and conduction bands obtained by using the first-order expression for the energy given by

$$m^* = \frac{4\pi\hbar^2}{3\sqrt{3}a\gamma_0L}. \quad (18)$$

It is noticed that upon multiplication by $\hbar^2\Omega^2$, the first term of equation (14) becomes independent of $\hbar\Omega$ and thus its derivative is zero. Therefore, the only nonzero contribution to the QEO response comes from the second term. Using equations (12) and (14) and inserting into equation (17), simple computations then yield

$$\begin{aligned} \chi''_{yy}(\omega; 0, 0, \omega) &= \frac{\sqrt{3}e^4a^3\gamma_0^3}{2\hbar^6\Omega^6L^2\epsilon_0} \sum_{\mu=0}^{N-1} \frac{|3\mu - n + m|}{(1 - \alpha^2)^{7/2}} \\ &\times \{3 \sin^{-1}(\alpha)(8\alpha^6 - 8\alpha^4 + 7\alpha^2 - 2) \\ &+ \alpha(1 - \alpha^2)^{1/2}(26\alpha^4 - 17\alpha^2 + 6)\}. \end{aligned} \quad (19)$$

This relatively simple equation allows us to compute analytically the QEO effect for semiconducting CNs with arbitrary (n, m) indices. For comparison, we illustrate the imaginary and real parts of $\chi^{(3)}(\omega; 0, 0, \omega)$ for some semiconducting CNs using the analytic expression equation (19) and a full numerical calculation in figures 4(a) and (b). The numerical calculation

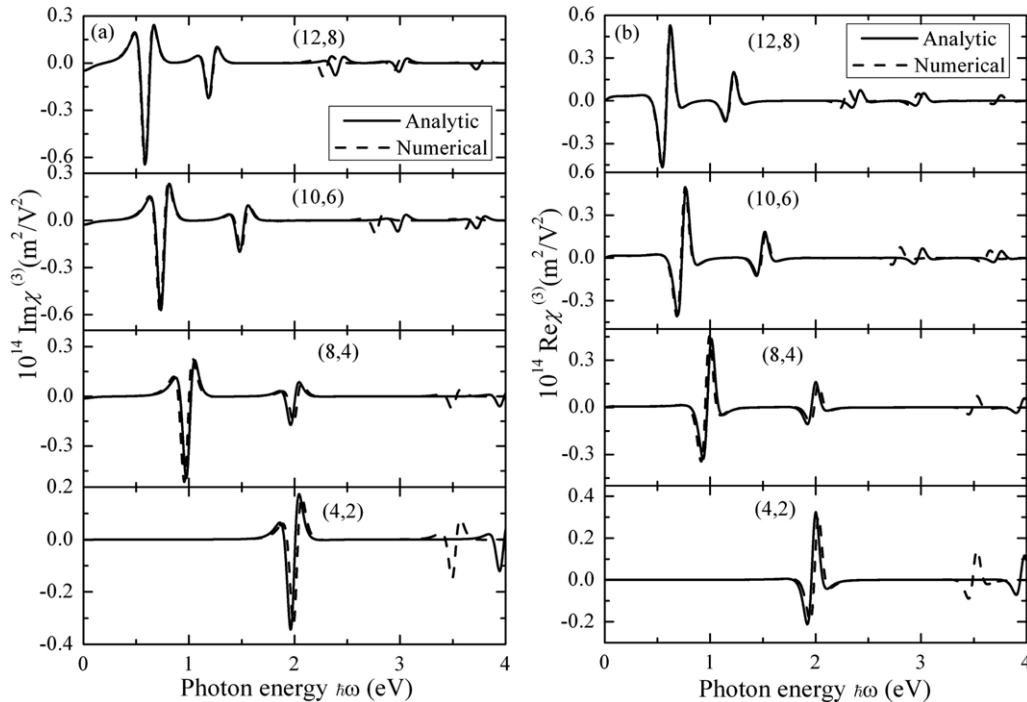


Figure 4. Comparison of analytic and numerical results for imaginary (a) and real (b) part of the QEO response for several semiconducting CNs.

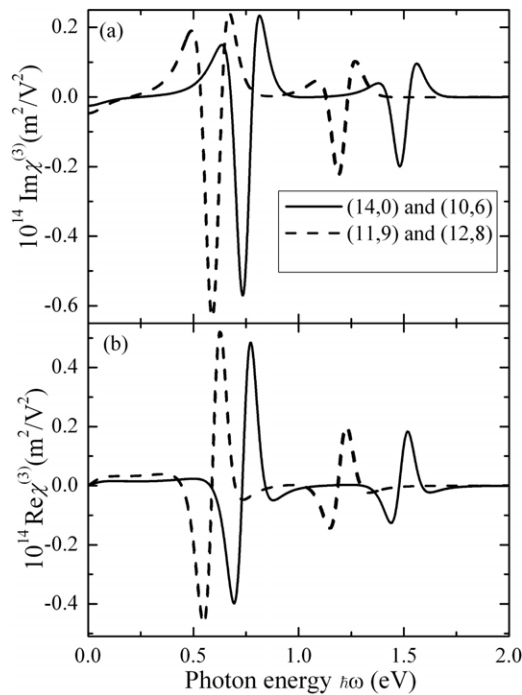


Figure 5. Imaginary (a) and real (b) part of the QEO response for several semiconducting CNs having the same diameter but different chirality.

is obtained by utilizing the perturbation treatment in [23] and using equations (8) and (17). To do this, we take account of the full k -dependence of transition energies and dipole matrix elements as well as include all band-to-band transitions and finally integrate over the first Brillouin zone numerically. As for the linear susceptibility, excellent agreement is observed for the first two resonance peaks for semiconducting CNs having a moderate or large diameter.

We compare the QEO effect for SI and SII CNs including (14, 0) and (10, 6) having the same diameter (1.09 nm) but different chirality $\theta = 30^\circ, 8.2^\circ$ and (11, 9) and (12, 8) having the same diameter (1.3 nm) but different chirality $\theta = 3.3^\circ, 6.6^\circ$, respectively. As shown in figure 5, the QEO effect at low energy for SI and SII CNs is virtually independent of the chirality and the type of SI or SII CNs as well. The QEO function depends weakly on chirality via the parameter ε_μ as demonstrated above for semiconducting CNs. Moreover, the effective mass in the denominator of the QEO function depends only on the nanotube diameter, see equation (18). As a result we get exactly the same spectrum for (14, 0) and (10, 6) CNs and also exactly the same spectrum for (11, 9) and (12, 8) CNs. By analyzing the fundamental resonance of several chiral CNs we have found a monotonous increase in the magnitude with increasing radius.

5. Summary

In this paper, we have derived an approximate analytic expression for long-axis linear susceptibility of CNs valid

for arbitrary diameter and chirality. Excellent agreement with full numerical calculations has been demonstrated in the low-photon energy range, in particular for semiconducting CNs. We have subsequently applied the general expression for the linear susceptibility to find an analytic expression for the quadratic electro-optic (QEO) effect in arbitrary (n, m) semiconducting CNs in good agreement with numerical results.

Acknowledgments

AZ is grateful to the Department of Physics and Nanotechnology, Aalborg University, Denmark and acknowledges support by the Ministry of Science, Research and Technology, Iran Grant No. 24/791052.

References

- [1] Saito R, Dresselhaus G and Dresselhaus M S 1998 *Physical Properties of Carbon Nanotubes* (London: Imperial College Press)
- [2] Samsonidze Ge G, Saito R, Kobayashi N, Grüneis A, Jiang J, Jorio A, Chou S G, Dresselhaus G and Dresselhaus M S 2004 *Appl. Phys. Lett.* **85** 5703
- [3] Jorio A, Fantini C, Pimenta M A, Capaz R B, Samsonidze Ge G, Dresselhaus G, Dresselhaus M S, Jiang J, Kobayashi N, Grüneis A and Saito R 2005 *Phys. Rev. B* **71** 075401
- [4] Iijima S 1991 *Nature* **345** 56
- [5] Mintmire J W, Dunlap B I and White C T 1992 *Phys. Rev. Lett.* **68** 631
- [6] Charlier J C and Lambin Ph 1998 *Phys. Rev. B* **57** R15037
- [7] Meunier V and Lambin Ph 1998 *Phys. Rev. Lett.* **81** 5588
- [8] Saito R, Dresselhaus G and Dresselhaus M S 2000 *Phys. Rev. B* **61** 2981
- [9] Popov V N and Henrard L 2004 *Phys. Rev. B* **70** 115407
- [10] Tasaki S, Maekawa K and Yamabe T 1998 *Phys. Rev. B* **57** 9301
- [11] Slepian G Ya, Maksimenko S A, Lakhtakia A, Yevtushenko O and Gusakov A V 1999 *Phys. Rev. B* **60** 17136
- [12] Lin M F and Shung K W K 1994 *Phys. Rev. B* **50** 17744
- [13] Ichida M, Mizuno S, Saito Y, Kataura H, Achiba Y and Nakamura A 2002 *Phys. Rev. B* **65** 241407
- [14] Li Z M, Tang Z K, Liu H J, Wang N, Chan C T, Saito R, Okada S, Li G D, Chen J S, Nagasawa N and Tsuda S 2001 *Phys. Rev. Lett.* **87** 127401
- [15] Zarifi A and Pedersen T G 2006 *Phys. Rev. B* **74** 155434
- [16] Mali'c E, Hirtshulz M, Milde F, Knorr A and Reich S 2006 *Phys. Rev. B* **74** 195431
- [17] White C T and Mintmire J W 1998 *Nature* **394** 29
- [18] Mintmire J W and White C T 1998 *Phys. Rev. Lett.* **81** 2506
- [19] Jiang J, Saito R, Grüneis A, Dresselhaus G and Dresselhaus M S 2004 *Carbon* **42** 3169
- [20] White C T, Robertsen D H and Mintmire J W 1993 *Phys. Rev. B* **47** 5485
- [21] Mintmire J W, Robertsen D H and White C T 1993 *J. Phys. Chem. Solids* **54** 1835
- [22] White C T and Mintmire J W 2005 *J. Phys. Chem. B* **109** 52
- [23] Aspnes D E and Rowe J E 1972 *Phys. Rev. B* **5** 4022
- [24] Zarifi A, Fisker C and Pedersen T G 2007 *Phys. Rev. B* **76** 045403